Late stage erythroid precursor production is impaired in mice with chronic inflammation

Olivier D. Prince,[1,2] Jacqueline M. Langdon,[1] Andrew J. Layman,[1] Ian C. Prince,[1] Miguel Sabogal,[1] Howard H. Mak,[3,4] Alan E. Berger,[5] Chris Cheadle,[5] Francis J. Chrest,[6] Qilu Yu,[1,7] Nancy C. Andrews,[3,8] Qian-Li Xue,[1] Curt I. Civin,[9] Jeremy D. Walston,[1] and Cindy N. Roy[1,3]

[1]Division of Geriatric Medicine and Gerontology, Johns Hopkins University School of Medicine, Baltimore, MD, USA; [2]Current address: Department of Acute Geriatrics, Townhospital Waid, Zurich, Switzerland; [3]Division of Hematology/Oncology, Children's Hospital Boston, Boston, MA, USA; [4]*Current address: Global Imaging, Novartis Institutes for BioMedical Research (NIBR), Cambridge, MA, USA*; [5]Lowe Family Genomics Core, Johns Hopkins University School of Medicine, Baltimore, MD, USA; [6]Rheumatic Disease Research Flow Cytometry Core Center, Johns Hopkins School of Medicine, Baltimore, MD; [7]*Current address: Westat, Rockville, MD, USA*; [8]*Current address: Department of Pediatrics and Department of Pharmacology and Cancer Biology, Duke University Medical Center, Durham, NC, USA*, and [9]Center for Stem Cell Biology and Regenerative Medicine and Department of Pediatrics, University of Maryland, Baltimore, MD, USA

Citation: Prince OD, Langdon JM, Layman AJ, Prince IC, Sabogal M, Mak HH, Berger AE, Cheadle C, Chrest FJ, Yu Q, Andrews NC, Xue Q-L, Civin CI, Walston JD, and Roy CN. Late stage erythroid precursor production is impaired in mice with chronic inflammation. Haematologica 2012;97(11):1648-1656. doi:10.3324/haematol.2011.053397

Online Supplementary Design and Methods

Animal care

Mice were housed in ventilated racks (Allentown Caging Equipment) with a 14-hour light cycle at the Johns Hopkins University barrier facility. Food and water were provided *ad libitum* until 16 h before sacrifice, at which point the mice were transferred to a clean cage and fasted overnight with only water available *ad libitum*.

Turpentine-induced sterile abscess

Turpentine oil (0.1 mL) was injected into the subcutaneous intrascapular region of female C57BL/6 mice at 5 to 7 weeks of age. The injection site was infiltrated by leukocytes, forming an abscess. To maintain an abscess in our model, mice were injected once weekly in the same location for 3 weeks with 0.1 mL turpentine oil. One week after the final injection, at 8 to 10 weeks of age, the mice were euthanized with no outward evidence of morbidity or cachexia.

Enzyme-linked immunosorbent assays

Whole blood was collected from the retro-orbital sinus into microtainer serum separator tubes (Becton Dickinson, Franklin Lakes, NJ, USA) from mice anesthetized with Avertin. Serum was separated and immediately stored at -80°C in single use aliquots. Samples were assayed from at least two independent experiments. The samples were thawed once, and then analyzed for serum iron or cytokines.

Weight and complete blood count

Female, 8- to 10-week old mice were anesthetized with an intraperitoneal injection of Avertin (125-240 mg/kg) and then weighed. We collected blood from the retro-orbital sinus into EDTA-treated microtainer tubes (Becton Dickinson) in order to determine the complete blood count. The mice were then euthanized with compressed carbon dioxide and tissues were collected for non-heme iron assay.

Gene expression

For mice which were sacrificed for RNA analyses, only 50 μL of blood were collected to verify complete blood count data and mice were sacrificed by cervical dislocation under Avertin anesthesia to reduce the possibility of hypoxic regulation of gene expression. Spleens were dissected and then cut with scissors into small pieces. The pieces were incubated at 37°C in 1X RPMI (Invitrogen, Carlsbad, CA, USA) with 0.05% collagenase (Sigma, St. Louis, MO, USA) and 0.002% DNase (NEBiolabs, Ipswich, MA, USA) for 35 min with agitation. Splenocytes were placed on ice and fetal bovine serum was added to a concentration of 5%. Splenocytes were washed and incubated at 4°C with rat anti-mouse F4/80 antibody (clone BM8, rat IgG2a, Invitrogen), followed by incubation with goat anti-rat IgG microbeads (Miltenyi, Auburn, CA, USA). F4/80+ splenic macrophages were positively selected on MACS columns (Miltenyi).

Total RNA was isolated from mouse livers or splenic macrophages by the Lowe Family Genomics Core facility using the Trizol reagent method according to the manufacturer's directions (Invitrogen). The quality of total RNA samples was assessed using an Agilent 2100 Bioanalyzer (Agilent Technologies, Columbia, MD, USA). Reverse transcription was performed by using total RNA isolated from mouse tissues and processed with the Applied Biosystems (Foster City, CA, USA) High-Capacity cDNA Archive kit first-strand synthesis system for reverse transcriptase polymerase chain reaction (RT-PCR) according to the manufacturer's protocol.

Probes and primers were designed and synthesized by Applied Biosystems: mu_Gapdh (Mm99999915_g1); mu_Actb (Mm00607939_s1); mu_Pgk1 (Mm00435617_m1); mu_Slc40a1 (mu_Ferroportin) (Mm00489837_m1); mu_Mfsd7b (mu_Feline leukemia virus subgroup c receptor) (Mm00816641_s1); mu_Slc48a1 (mu_Heme regulated gene-1) (Mm00728070_s1); mu_Hamp1 (mu_Hepcidin) (Mm00519025_m1); mu_Tmprss6 (mu_Transmembrane serine protease 6) (Mm00551108_m1); mu_Bmp6 (mu_Bone morphogenetic protein 6) (Mm01332882_m1); mu_Id1 (mu_Inhibitor of DNA binding 1)

(Mm00775963_g1). The TaqMan® probes and primers for hepcidin are expected to amplify endogenous hepcidin mRNA as well as the transgenic hepcidin mRNA. Relative gene expressions and *P* values were calculated using the $2^{-\Delta\Delta Ct}$ method.[1] The normalized ΔC_t value of each sample was calculated using a total of three endogenous control genes (*Gapdh*, *Actb*, and *Pgk1*). Fold change values were obtained by computing $2^{-(average\Delta\Delta Ct)}$ for genes in "trial" relative to control samples. The endpoints of error bars were at the fold changes $2^{-(average\Delta\Delta Ct \pm SEM)}$ where SEM is the standard error of the mean for $\Delta\Delta C_t$ calculated from the ΔC_t values from samples with four to eight mice in each group.

Immunoblotting

Post-translational regulation of ferroportin was assessed by immunoblotting, essentially as described previously.[2] F4/80+ splenic macrophages were isolated as described in the main *Design and Methods* section for gene expression analyses. Cell pellets were lysed and membrane fractions were prepared using the Qiagen Qproteome Plasma Membrane Protein kit (Qiagen, Valencia, CA, USA) according to the manufacturer's instructions. Subcellular fractions were separated on NuPAGE Bis Tris gels using MOPS buffer (Life Technologies, Grand Island, NY, USA) and transferred to a Protran nitrocellulose membrane (Whatman/Perkin Elmer, Boston, MA, USA). Blots were probed with rabbit anti-mouse ferroportin (1:1500, Novus Biologicals, Littleton, CO, USA) or mouse anti-actin (1:500, Sigma-Aldrich, St. Louse, MO, USA), followed by corresponding horseradish peroxidase-linked secondary antibodies (GE Healthcare, Piscataway, NJ, USA). Blots were developed with a chemiluminescent substrate (Supersignal West Dur, Thermo Scientific, Rockford, IL, USA) and exposed to Hyper Film (GE Healthcare). Protein expression was quantified using Quantity One software (Biorad, Hercules, CA, USA). The adjusted volume was obtained by measuring the intensity per mm^2 of each band relative to background signal. Numerical values of ferroportin protein are calculated by dividing the ferroportin values by the actin values for each sample.

Flow cytometry and oxidative stress

Briefly, mouse bone marrow was flushed from the femur using RPMI with 2.5% heat inactivated fetal bovine serum. The clumps were dispersed with an 18-gauge needle and stained with antibodies to Ter119, CD45, CD71, and/or CD44 (BD Pharmingen, Franklin Lakes, NJ, USA). The cell staining was quantified with the FACS Calibur (Beckton Dickinson). Flow cytometry plots are from one representative mouse in each group. Data are representative of at least two independent experiments with three to five mice in each group.

Results

Gene and protein expression changes in splenic macrophages are consistent with extramedullary hematopoiesis and serum iron concentration

The spleens of mice with sterile abscesses were nearly double the size of those from controls, which indicated extramedullary erythropoiesis was occurring. To assess whether erythropoiesis was, in fact, occurring in the spleen, we looked for erythroid precursors in splenocyte preparations isolated from mice with sterile abscesses, hepcidin Tg+ mice and controls (*Online Supplementary Figure S1A-C*). We used antibodies to assess stage-specific markers of erythropoiesis to analyze erythroid precursor maturation by flow cytometry, resolving erythroid precursors by Ter119 and CD44 staining as previously described.[3,4] We found significant numbers of erythroid precursors in spleens of mice with sterile abscesses (*Online Supplementary Figure S1B*), but essentially no erythroid precursors could be found in control spleens (*Online Supplementary Figure S1A*) or hepcidin Tg+ spleens (*Online Supplementary Figure S1C*).

To compare the role of splenic macrophages in iron handling in these two mouse models, we analyzed the expression of the heme exporter, *feline leukemia virus subgroup C receptor* (*Mfsd7b*); the intracellular heme transporter, *heme regulated gene-1* (*Slc48a1*); *heme oxygenase 1* (*Hmox1*); and the transporter responsible for elemental iron egress, *ferroportin* (*Slc40a1*) in F4/80+ splenic macrophages of mice with sterile abscesses, hepcidin Tg+ mice, and controls. *Hmox1* expression was unchanged (*data not shown*). *Slc48a1* expression was increased 2.5-fold in splenic macrophages of mice with abscesses (P=0.001, *Online Supplementary Figure S1D*). We found that the mRNA expression of *Slc40a1* was elevated 2.8-fold (P=0.003) in mice with abscesses and 1.8-fold (P=0.03) in hepcidin Tg+ mice (*Online Supplementary Figure S1D*).

To determine the steady state expression of ferroportin in splenic macrophages, we assessed ferroportin expression in the membranes of splenic macrophages by immunoblotting (*Online Supplementary Figure S1E*). We found that ferroportin was lowest in the hepcidin Tg+ mice (*Online Supplementary Figure S1E*, lanes 7-9; *Online Supplementary Figure S1F*, dark gray bars, median membrane ferroportin/actin ratio=1.68; range, 1.32-5.61), consistent with hepcidin expression from the transgene and their low serum iron concentration. Ferroportin expression was somewhat higher in mice with abscesses than in hepcidin Tg+ mice (*Online Supplementary Figure S1E*, lanes 4-6; *Online Supplementary Figure S1F*, white bars, median membrane ferroportin/actin ratio=2.39; range, 1.50-4.83). In general, the expression was lower in both groups than in the control group (*Online Supplementary Figure S1E*, lanes 1-3; *Online Supplementary Figure S1F,* black bars, median membrane ferroportin/actin ratio=4.61; range, 2.34-5.29). Thus, membrane-associated ferroportin expression in splenic macrophages was consistent with serum iron concentration in hepcidin Tg+ mice, but not in mice with sterile abscesses.

Discussion

We observed extramedullary hematopoiesis only in the mice with sterile abscesses, which might suggest mechanistic differences between erythrocyte production in the sterile abscess model *versus* the hepcidin Tg+ model. To investigate iron handling in splenic macrophages, we assessed the expression of mRNA encoding proteins important for heme export in splenic macrophages. While we did not find any change in *Hmox1* expression, we found that *Slc48a1* expression was increased 2.5-fold in splenic macrophages of mice with abscesses. The Hrg-1 protein was identified for its ability to transport heme in

the heme auxotroph *C. elegans*. Hrg-1 has been localized to intracellular vesicles of mammalian cells, but its specific role in heme trafficking remains under investigation.[5] To our knowledge, this is the first evidence of *Slc48a1* regulation in a vertebrate animal. These results may implicate Hrg-1 in phagosomal heme uptake of failed erythroid precursors that are recognized for removal by the central macrophage of erythroid islands. Increased *Slc48a1* mRNA is a unique feature of splenic macrophages in mice with abscesses. This finding may indicate more efficient recovery of iron from heme in mice with abscesses than in hepcidin Tg+ mice, or may simply be a physiological change consistent with extramedullary hematopoiesis.

Increased *Slc40a1* mRNA expression in mice with abscesses may be consistent with increased erythroid precursor turnover, as previously described for erythrophagocytosis in cultured macrophages,[6-8] although the functional importance of increased *Slc40a1* mRNA is unclear in the light of decreased membrane-associated ferroportin protein. Reduced membrane-associated ferroportin expression was somewhat unexpected in mice with sterile abscesses because hepcidin expression returns to baseline after 3 weeks of abscess. However, *hepcidin* mRNA expression may normalize before ferroportin protein expression normalizes. Additionally the splenic macrophages in mice with sterile abscesses are different because at least a subset support extramedullary hematopoiesis. Ferroportin may not be highly expressed in splenic macrophages of mice with sterile abscesses because macrophages which support extramedullary hematopoiesis in the spleen may be qualitatively different from those responsible for erythrophagocytosis and iron recycling. The F4/80 macrophage marker does not discriminate between central macrophages which support erythropoiesis and the macrophages responsible for erythrophagocytosis and iron recycling. Thus ferroportin expression normalized to the total number of splenic macrophages may under-represent iron egress activity in mice with sterile abscesses.

Despite low membrane-associated ferroportin expression in splenic macrophages of mice with sterile abscesses, serum iron concentrations were normal in these mice. It is important to note that if iron egress is decreased from splenic macrophages with less membrane-associated ferroportin in mice with sterile abscesses, this change in flux seems to be matched by reduced utilization by erythroid precursors. We have commented in the main text of the manuscript that serum iron levels may be normal because transferrin-bound iron utilization is suppressed with impaired erythrocyte development.

References

1. Yuan JS, Reed A, Chen F, Stewart CN, Jr. Statistical analysis of real-time PCR data. BMC Bioinformatics. 2006;7:85.
2. Vanoaica L, Darshan D, Richman L, Schumann K, Kuhn LC. Intestinal ferritin H is required for an accurate control of iron absorption. Cell Metab. 2010;12(3):273-82.
3. Chen K, Liu J, Heck S, Chasis JA, An X, Mohandas N. Resolving the distinct stages in erythroid differentiation based on dynamic changes in membrane protein expression during erythropoiesis. Proc Natl Acad Sci USA. 2009;106(41):17413-8.
4. Gardenghi S, Ramos P, Marongiu MF, Melchiori L, Breda L, Guy E, et al. Hepcidin as a therapeutic tool to limit iron overload and improve anemia in beta-thalassemic mice. J Clin Invest. 2010;120(12):4466-77.
5. Rajagopal A, Rao AU, Amigo J, Tian M, Upadhyay SK, Hall C, et al. Haem homeostasis is regulated by the conserved and concerted functions of HRG-1 proteins. Nature. 2008;453(7198):1127-31.
6. Delaby C, Pilard N, Hetet G, Driss F, Grandchamp B, Beaumont C, Canonne-Hergaux F. A physiological model to study iron recycling in macrophages. Exp Cell Res. 2005;310(1):43-53.
7. Knutson MD, Vafa MR, Haile DJ, Wessling-Resnick M. Iron loading and erythrophagocytosis increase ferroportin 1 (FPN1) expression in J774 macrophages. Blood. 2003;102(12):4191-7.
8. Knutson MD, Oukka M, Koss LM, Aydemir F, Wessling-Resnick M. Iron release from macrophages after erythrophagocytosis is up-regulated by ferroportin 1 overexpression and down-regulated by hepcidin. Proc Natl Acad Sci USA. 2005;102(5):1324-8.

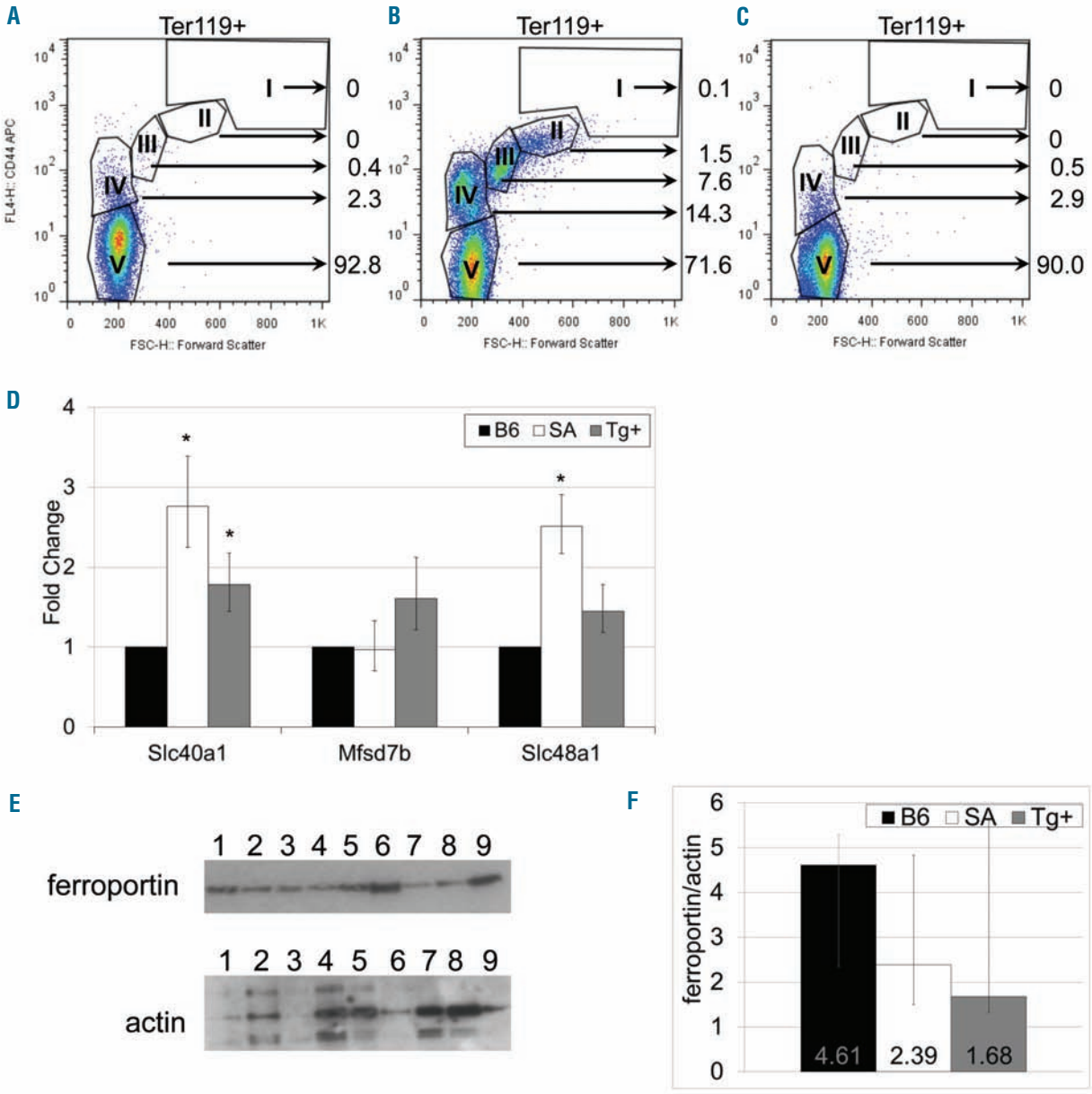

Online Supplementary Figure S1. Heme and iron transport genes are induced in splenic macrophages of mice with sterile abscesses. We assessed erythroid maturation in spleens of control mice (A), mice after 3 weeks of sterile abscesses (B), and hepcidin Tg+ mice (C). Total splenocytes were selected for Ter119 to define erythroid precursors (EP). Then Ter119$^+$ cells were further analyzed according to size (forward scatter) and CD44 expression. We only found early stage EP (gates II and III) in mice with sterile abscesses (B). All mice were females 8-10 weeks of age. Flow cytometry plots are from one representative mouse in each group. Data are representative of two independent experiments with three to five mice in each group. Splenic macrophages were isolated from collagenase-treated spleens of C57BL/6 controls (B6, black bars, n= 4), hepcidin Tg+ mice (Tg+, dark gray bars, n= 4) and C57BL/6 mice with sterile abscesses (SA, white bars, n= 4) using the rat anti-mouse F4/80 antibody and a MACS positive selection column (D). Quantitative PCR of cDNA from these macrophages revealed significantly increased expression of *Slc40a1* (P=0.003) and *Slc48a1* (P=0.001) in mice with sterile abscesses, indicated by asterisks. No significant change was observed for *Mfsd7b* across the groups. All mice were females 8-10 weeks of age. Membrane-associated ferroportin [top panel, (E)] was lowest in hepcidin Tg+ mice (lanes 7-9), as predicted by serum iron concentration. Membrane-associated ferroportin was highest in controls (lanes 1-3). Cytosolic actin is shown in the bottom panel. Data from three individual mice in each treatment group are presented. Individual immunoblot images represent contiguous lanes of the blot and were scanned and densitometry was performed using Quantity One software, normalizing ferroportin to actin (F). Bars represent the median and error bars represent the range of the ratio for each group of mice. Adjustments of brightness and contrast were made to the entire blot to match the original film. No information from the original film was obscured, eliminated or misrepresented.